

Neutron Diffraction Investigation of Ordered Oxygen Vacancies in the Defect Pyrochlores, $\text{Pb}_2\text{Ru}_2\text{O}_{6.5}$ and $\text{PbTiNb}_2\text{O}_{6.5}$

R. A. BEYERLEIN,¹ H. S. HOROWITZ, J. M. LONGO,
AND M. E. LEONOWICZ

*Exxon Research and Engineering Co., Corporate Research Labs,
Annandale, New Jersey 08801*

AND J. D. JORGENSEN² AND F. J. ROTELLA²

Argonne National Laboratory, Argonne, Illinois 60439

Received July 25, 1983

Powder neutron diffraction has been used to investigate the structure of the defect pyrochlores $\text{Pb}_2\text{Ru}_2\text{O}_{6.5}$ and $\text{PbTiNb}_2\text{O}_{6.5}$. Both materials show evidence for oxygen vacancy ordering that is accompanied by *A*-site cation displacement. The diffraction data for $\text{Pb}_2\text{Ru}_2\text{O}_{6.5}$ have been successfully fit in the cubic space group $F\bar{4}3m$. The results confirm half occupancy of the defect site, demonstrate oxygen vacancy ordering, and show that each Pb atom is displaced by 0.040(4) Å toward its associated vacancy. The diffraction data for $\text{PbTiNb}_2\text{O}_{6.5}$ have been fit in the tetragonal space group $P\bar{4}m2$ using a model that allows ordering of Pb and Ti on the *A* site in concert with oxygen vacancy ordering. The fitting results specify a stoichiometry $\text{PbTi}_{0.90}\text{Nb}_2\text{O}_{6.45}$ for this material; the slight Ti deficiency is probably associated with some Ti loss to the vessel walls during the sealed tube synthesis at 600°C. The Rietveld structural refinement also shows that Pb is displaced slightly away from its associated vacancy while Ti is displaced significantly toward its associated vacancy with resulting Ti-Ti separations similar to those found in Ti metal. It is suggested that the *A*-site cation ordering observed in each of these materials is a consequence of *A* cation-oxygen bonding rather than the formation of *A*-*A* bonds through the oxygen vacancy despite the close *A*-*A* separations observed. These results are believed to provide the first examples of anion/vacancy ordering in a defect pyrochlore of the type $\text{A}_2\text{B}_2\text{O}_{7-y}$.

Introduction

Recent results concerning the use of oxide pyrochlores of the form $\text{Pb}_2(\text{Ru}_{2-x}\text{Pb}_x^{4+})\text{O}_{6.5}$ (1), $0 \leq x \leq 1$, as bidirectional electrocatalysts for both O_2 reduction and evolution (2) and as catalysts for electroorganic oxidation (3) suggest that the catalytic activity of these materials is related to their oxygen nonstoichiometry. Al-

though the $x = 0$ end member of the above series was originally suggested to be $\text{Pb}_2\text{Ru}_2\text{O}_7$ by Randall and Ward (4) and was later reported as $\text{Pb}_2\text{Ru}_2\text{O}_6$ by Longo *et al.* (5), recent investigation (1) has shown the correct stoichiometry to be $\text{Pb}_2\text{Ru}_2\text{O}_{6.5}$. A preliminary neutron powder diffraction investigation of this material confirmed this stoichiometry while at the same time demonstrating that the vacancies are ordered (6). The Rietveld structural refinement also showed that each Pb atom is slightly displaced toward its associated vacancy.

¹ To whom correspondence should be addressed.

² Work supported in part by the U.S. Department of Energy.

These initial results suggested that oxygen vacancy ordering with associated *A*-site cation ordering may be a frequently encountered phenomenon for oxygen defect pyrochlores of the form $A_2B_2O_{7-y}$, $y \approx \frac{1}{2}$, when the *A*-site is occupied by a post-transition metal cation having an easily polarizable $6s^2$ electron pair such as Tl^+ , Pb^{2+} , or Bi^{3+} . A new oxygen defect pyrochlore, $PbTiNb_2O_{6.5}$, has been prepared in order to further investigate vacancy ordering of this type. In this paper the results of a neutron diffraction investigation of this material are reported as well as a more complete account of our recent investigation of oxygen vacancy ordering in $Pb_2Ru_2O_{6.5}$ (6).

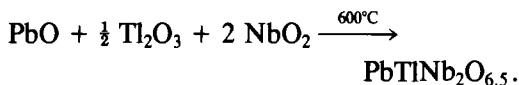
Writing the general pyrochlore formula as $A_2O' \cdot B_2O_6$ emphasizes the fact that this structure may be viewed as two interpenetrating networks (7). The *B* cations are located at the center of corner sharing oxygen (O) octahedra that form a system of interconnected cages. The special oxygen O' , located at the center of these cages, may be partially or totally absent and is therefore associated with the anion nonstoichiometry observed in pyrochlores. The A_2O' sublattice may be viewed either as a system of intersecting $-A-O'-A-O'-$ zigzag chains (cuprite structure) or as a network of corner-sharing A_4O' tetrahedra. In the random vacancy model for oxygen defect pyrochlores, $A_2B_2O_{7-y}$, $0 < y \leq 1$, each O' site is fractionally occupied.

Experimental

The $Pb_2Ru_2O_{6.5}$ sample was prepared by solid state reaction in a manner similar to a procedure previously described (1, 5). Powder X-ray diffraction showed a single-phase pyrochlore with a unit cell edge of $a_0 = 10.252(1)$ Å. Thermogravimetric reduction in hydrogen gave a formula $Pb_2Ru_2O_{6.5 \pm 0.04}$. Time-of-flight neutron diffraction data were collected at the High Resolution Powder Diffractometer (HPRD)

at Argonne's ZING P' (8) pulsed neutron source using the $2\theta = 160^\circ$ detector bank. Data collection required about 52 hr of machine time for a 4-cm³ powder sample.

The $PbTiNb_2O_{6.5}$ sample was prepared by reacting PbO , Tl_2O_3 , and NbO_2 at 600°C for 115 hr in a sealed, evacuated quartz tube as follows:



NbO_2 was separately prepared by reducing Nb_2O_5 with Nb metal in a sealed, evacuated quartz tube at 1000°C for 40 hr. Powder X-ray diffraction showed a single-phase pyrochlore, mustard-brown in color, with $a_0 = 10.63(1)$ Å. Time-of-flight neutron diffraction data were collected at the Special Environment Powder Diffractometer (SEPD) at Argonne's IPNS-I pulsed neutron source. Data collection required about 15 hr. A full description of the diffractometers (HPRD and SEPD) and the Rietveld refinement software used to analyze the data has been given elsewhere (9-12).

Results and Discussion

(1) $Pb_2Ru_2O_{6.5}$

The data were first refined in the pyrochlore space group $Fd\bar{3}m$, (O_h^7 , No. 227, origin at $\bar{3}m$) with atoms at positions: Pb, 16c; Ru, 16d; O, 48f; special oxygen O' at 8a. The refinement included 2018 data points, 437 allowed reflections and 19 refined parameters, including the cubic cell constant, occupation factors, and full anisotropic thermal parameters for all atoms. The fitted region included all *d*-spacings between 0.41 and 2.40 Å. The weighted *R* value calculated point by point with background included was 3.99% while the Rietveld *R*, calculated after removing the background, was 6.06%. The final refined oxygen position parameter was $x_0 = 0.4268(1)$ in agreement with the value determined previously

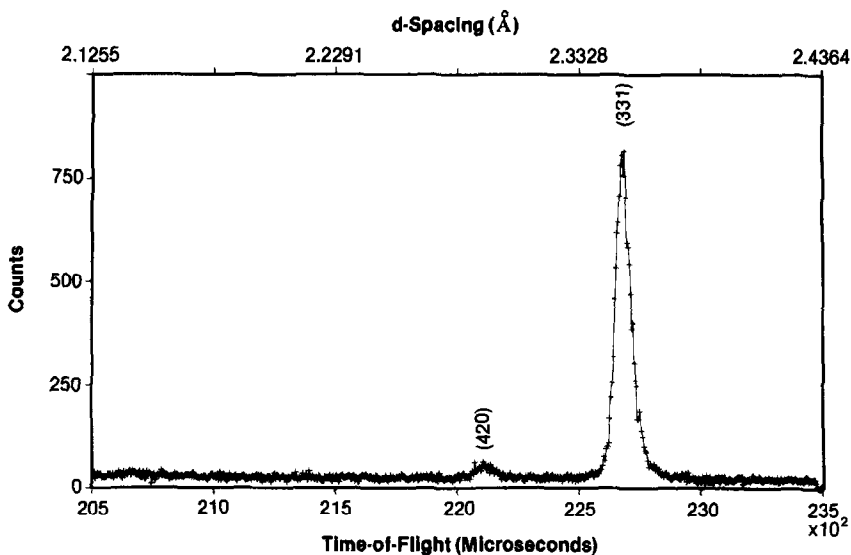


FIG. 1. Raw TOF neutron diffraction data showing (420) and (331) reflections for $\text{Pb}_2\text{Ru}_2\text{O}_{6.5}$.

by X-ray diffraction (5), $x_0 = 0.429(3)$. The refined fractional occupancy of the anion defect site, O' at $8a$, was $0.50(1)$, in excellent agreement with the stoichiometry determined from the thermogravimetric data.

While our initial refinement appeared successful, close examination of both the neutron and the powder X-ray data showed several weak lines of the type $hk0$ with $h + k = 2n$; such reflections are forbidden in $Fd\bar{3}m$. The weak (420) reflection present in the neutron data (Fig. 1) and the (420) and (640) reflections observed in the X-ray data are consistent with the loss of inversion symmetry at the cation sites, a result that would occur if the oxygen vacancies were ordered. A second refinement was performed using the space group $F\bar{4}3m$ (T_d^2 , No. 216), the space symmetry that results when the inversion constraint in $Fd\bar{3}m$ is relaxed in order to allow oxygen vacancy ordering. This space group also allows cation displacement along [111]. The weighted profile R -value in this refinement improved to 3.63%. Refined values for the position, thermal, and occupation parameters are

given in Table I, and the best fit profile is shown in Fig. 2. For the oxygen atoms O_1 and O_2 forming the octahedral cage around each Ru, the Ru—O bond lengths are $1.954(4)$ and $1.969(4)$ Å, respectively; these values agree with the Ru—O bond length in $Fd\bar{3}m$, $1.961(1)$ Å, within 2 standard deviations. The occupation parameter for the special oxygen O' at $4d$ refined to a value $0.96(2)$ with the alternative oxygen defect site at $4a$ vacant. This yields a stoichiometry parameter for the O' site of $0.48(1)$. The refined values for the Pb and Ru atom positions at $16e$ (x, x, x), $x_{\text{Pb}} = 0.8772(2)$ and $x_{\text{Ru}} = 0.3754(2)$, show that Pb has been displaced significantly farther from the $Fd\bar{3}m$ inversion symmetry position, $x_{\text{Pb}} = 0.875$, than has the Ru atom, which is within 2 standard deviations of $x_{\text{Ru}} = 0.375$. As shown in Fig. 3, each Pb atom is displaced by $0.040(4)$ Å toward its associated vacancy so that, along the [111] direction, the Pb-vacancy distance is $2.180(2)$ Å while the Pb— O' distance is $2.260(2)$ Å. These results show that the anion vacancies in $\text{Pb}_2\text{Ru}_2\text{O}_{6.5}$ are ordered with an associated ordering of the Pb cations.

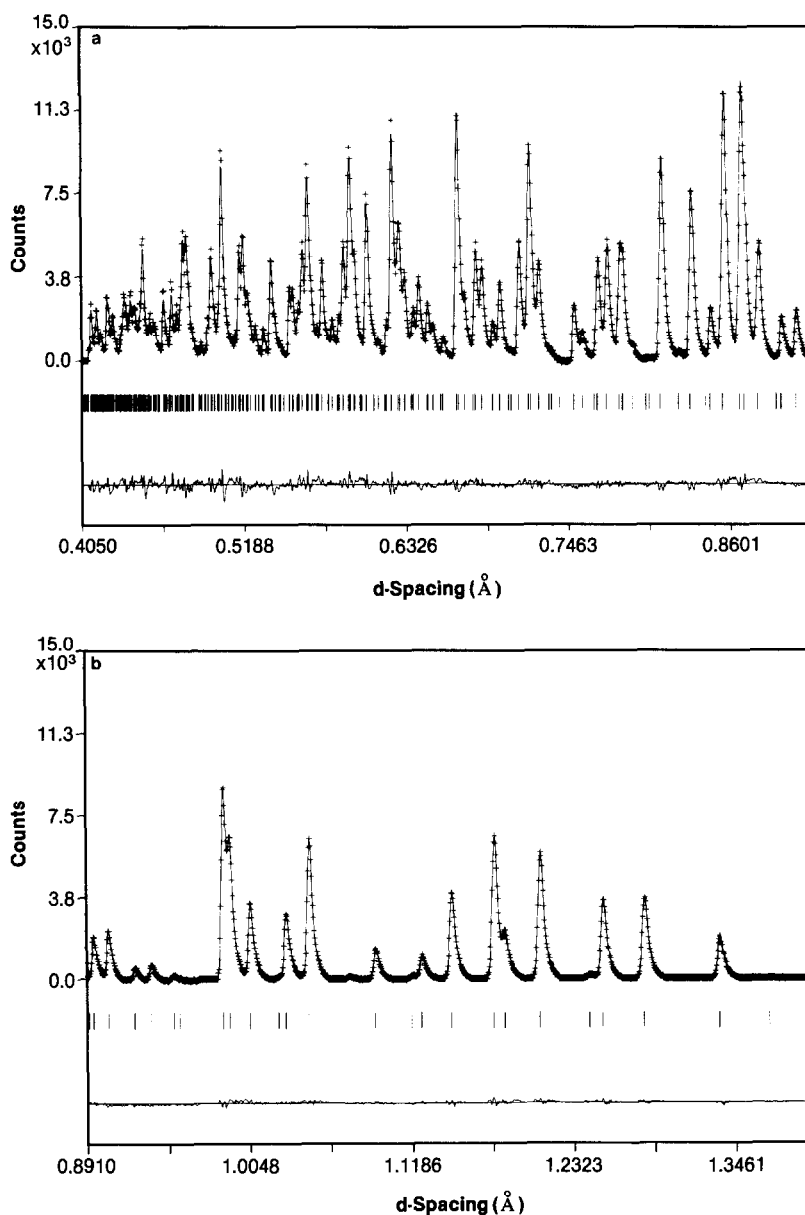


FIG. 2. (a,b,c,d) Refinement profile for $\text{Pb}_2\text{Ru}_2\text{O}_{6.5}$ in $F\bar{4}3m$ (No. 216, origin at $\bar{4}3m$). Plus marks (+) are the raw data points. The solid line is the best-fit profile. A difference (observed - calculated) appears at the bottom. Tick marks below a profile indicate the positions of all allowed reflections included in the calculation. Background has been removed prior to plotting.

Attempts to synthesize $\text{Pb}_2\text{Ru}_2\text{O}_6\text{F}$ in order to demonstrate extinction of the (420) reflection when vacant anion sites are filled were unsuccessful (13).

(2) $\text{PbTiNb}_2\text{O}_{6.5}$

All diffraction patterns for $\text{PbTiNb}_2\text{O}_{6.5}$ can be fully indexed using a cubic lattice

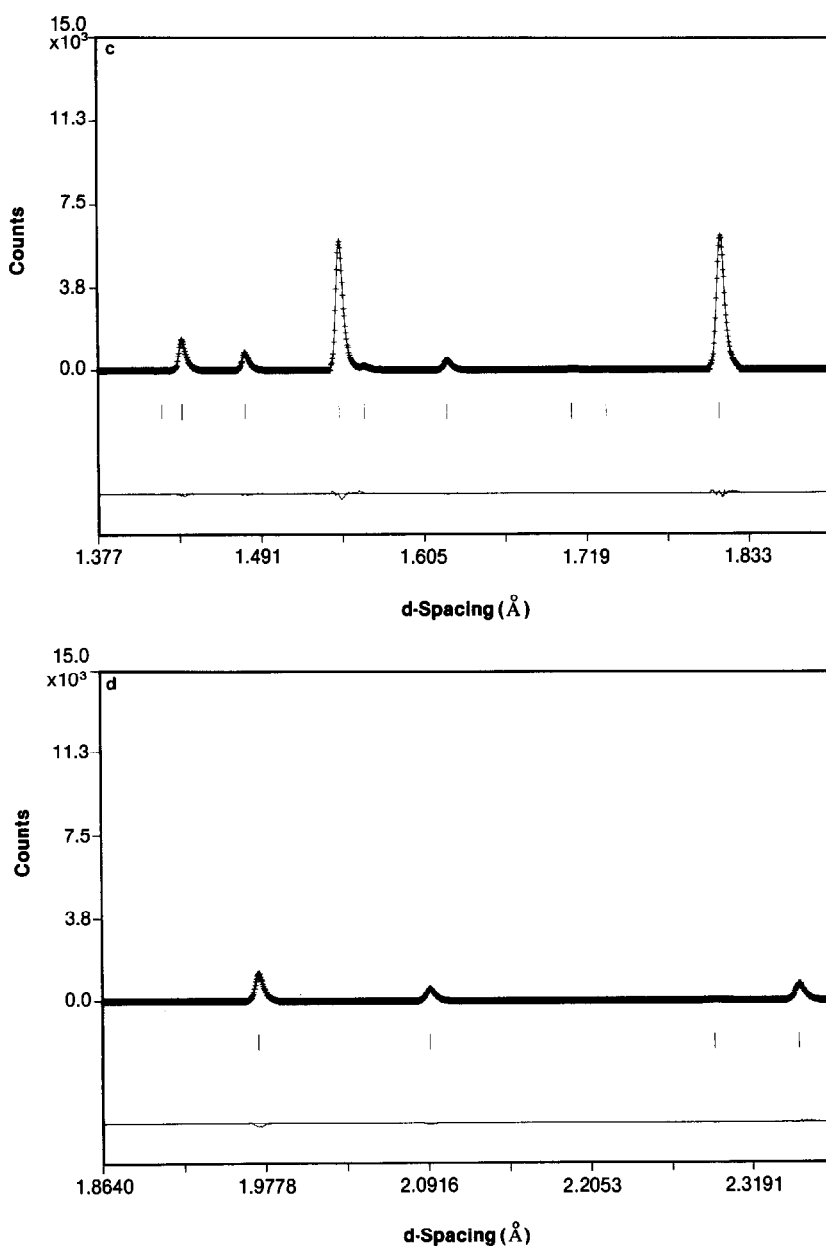


FIG. 2—Continued.

parameter, $a_0 = 10.623(3)$ \AA . This lattice parameter may be compared with those of several closely related defect pyrochlores, $\text{Ti}_2\text{Nb}_2\text{O}_6$ (14–16) with $a_0 = 10.60$ \AA and $\text{Pb}_{1.5}\text{Ta}_2\text{O}_{6.5}$ and $\text{Pb}_{1.5}\text{Nb}_2\text{O}_{6.5}$ (17–22) each with $a_0 = 10.56$ \AA . As was the case for

$\text{Pb}_2\text{Ru}_2\text{O}_{6.5}$, the X-ray diffraction pattern for $\text{PbTiNb}_2\text{O}_{6.5}$ shows a weak but definite (420) reflection (Fig. 4), again suggesting vacancy ordering. The neutron data, which also exhibit a (420) reflection, were first refined in the space group $F\bar{4}3m$ (T_d^2 , No.

TABLE I
STRUCTURAL PARAMETERS FOR $\text{Pb}_2\text{Ru}_2\text{O}_{6.5}$ IN $F\bar{4}3m$, ORDERED VACANCY MODEL

| $(a_0 = 10.2519(2) \text{ \AA}, R_{\text{weighted}} = 3.63\%, R_{\text{Rietveld}} = 5.43\%)$ | | | | | | |
|--|--------------|----------------|----------------|--------------|----------------|----------------------|
| Atom | Site | Stoichiometry | x^a | | | $B (\text{\AA}^2)^b$ |
| Pb | 16e (x,x,x) | 1.98(2) | 0.8772(2) | [7/8] | | 0.51(4) |
| Ru | 16e (x,x,x) | 1.93(2) | 0.3754(2) | [3/8] | | 0.18(3) |
| O ₁ | 24f (x,0,0) | 3 | 0.3028(2) | [0.3018(1)] | | 0.68(10) |
| O ₂ | 24g (x,½,½) | 3 | 0.4492(2) | [0.4482(2)] | | 0.50(10) |
| O' | 4d (¾,¾,¾) | 0.48(1) | ¾ | — | | 0.47(9) |
| Atom | β_{11} | β_{22} | β_{33} | β_{12} | β_{13} | β_{23} |
| Pb | 0.00124(4) | = β_{11} | = β_{11} | -0.00014(3) | = β_{12} | = β_{12} |
| Ru | 0.00044(3) | = β_{11} | = β_{11} | -0.00008(3) | = β_{12} | = β_{12} |
| O ₁ | 0.00159(16) | 0.00058(8) | = β_{22} | 0 | 0 | -0.00033(12) |
| O ₂ | 0.00121(12) | 0.00131(10) | = β_{22} | 0 | 0 | -0.00076(15) |
| O' | 0.00115(12) | = β_{11} | = β_{11} | 0 | 0 | 0 |

Note. The above refinement in $F\bar{4}3m$ employed 25 variable parameters and 2072 degrees of freedom. The comparable refinement for $Fd\bar{3}m$ (Random Vacancy Model) employed 19 variable parameters, 1999 degrees of freedom, and gave $R_{\text{weighted}} = 3.99\%$, $R_{\text{Rietveld}} = 6.06\%$.

^a Values in brackets are refined positions in $Fd\bar{3}m$ with a change of origin by $(\frac{1}{8}, \frac{1}{8}, \frac{1}{8})$ from $3m$. x_{O1} and x_{O2} are related by symmetry in $Fd\bar{3}m$.

^b B_{eff} (isotropic) = $B(\text{\AA}^2) = 4a_0^2\beta_{11}$.

216), with Pb and Tl disordered on the A-site at 16e. The refinement included 2403 allowed data points, 179 allowed reflections, and 18 refined parameters including the cubic cell constant, occupation factors for {Pb, Tl} and O' and isotropic tempera-

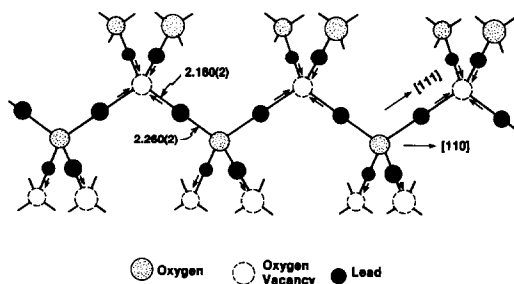


FIG. 3. $\text{Pb}_2\text{O}_{0.5}$ sublattice in the ordered vacancy model for $\text{Pb}_2\text{Ru}_2\text{O}_{6.5}$, $F\bar{4}3m$. Arrows indicate the directions of displacement of each Pb atom with respect to the A-site position in $Fd\bar{3}m$. Distances are given in Ångstroms.

ture factors for all atoms. The weighted profile R value was 5.00% and the Rietveld R was 10.27%. The refinement results are summarized in Table II. The Nb—O bond lengths are 2.00(1) and 1.98(1) Å, respectively, and are very similar to the Nb—O bond length of 2.01(2) Å in $\text{Ti}_2\text{Nb}_2\text{O}_6$ (16) or 1.97 Å in $\text{Pb}_{1.5}\text{Nb}_2\text{O}_{6.5}$ (21, 22). The {Pb, Tl} ion on the A-site is displaced toward the oxygen vacancy by

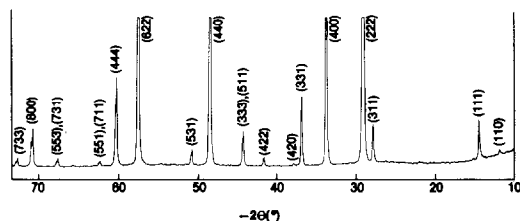


FIG. 4. X-Ray diffraction pattern for $\text{PbTiNb}_2\text{O}_{6.5}$. Indexing is done using a cubic lattice parameter $a_0 = 10.623(3) \text{ \AA}$.

TABLE II
STRUCTURAL PARAMETERS FOR $\text{PbTiNb}_2\text{O}_{6.5}$ IN
 $F43m$ WITH ORDERED OXYGEN VACANCIES,
DISORDERED Pb, Ti

| $(a_0 = 10.6225(1) \text{ \AA}, R_{\text{weighted}} = 5.00\%,$ $R_{\text{Rietveld}} = 10.27\%, R_{\text{expected}} = 2.07\%)$ | | | | |
|--|--|---------------|-----------|---------------------------|
| Atom | Site | Stoichiometry | x | B (\AA^2) |
| Pb | 16e (x,x,x) | 0.96(1) | 0.8792(4) | 1.83(6) |
| Ti | 16e (x,x,x) | 0.96(1) | 0.8792(4) | 1.83(6) |
| Nb | 16e (x,x,x) | 2 | 0.3745(4) | 0.76(6) |
| O ₁ | 24f (x,0,0) | 3 | 0.3118(3) | 0.54(2) |
| O ₂ | 24g (x, $\frac{1}{2}$, $\frac{1}{2}$) | 3 | 0.4357(4) | 1.03(5) |
| O ₃ | 4d ($\frac{1}{2}$, $\frac{1}{2}$, $\frac{1}{2}$) | 0.46(2) | — | 2.2 (2) |
| O ₄ | 4a (0,0,0) | 0 | — | — |

0.08(1) \AA . In a subsequent refinement, the oxygen on the defect site was initially distributed equally on sites 4d and 4a, with the oxygen stoichiometries for these sites constrained so as to sum to $\frac{1}{2}$. Only 10% of this $\frac{1}{2}$ oxygen per formula unit remained on the vacancy site at 4a, and all other parameters remained essentially unchanged. While the fit in $F43m$ appears to substantiate the ordering of the oxygen vacancies with associated cation displacement, the model is inadequate in that it cannot differentiate between Pb and Ti atoms. Thus, the resulting requirement that Pb and Ti are displaced by equal amounts is clearly artificial. In addition, close examination of the powder X-ray data shows a weak but definite (110) reflection (Fig. 4) that clearly violates F -centering extinction conditions. These observations suggest that there is ordering of Pb and Ti on the A-site in addition to oxygen vacancy ordering.

Pb and Ti cannot be ordered in any cubic space group in which these atoms fully occupy two distinct crystallographic sites. We considered a model in which $\frac{1}{4}$ of the anion defect sites are coordinated by 4 Ti atoms, $\frac{1}{4}$ by 4 Pb atoms, and the remaining $\frac{1}{2}$ of the defect sites are coordinated by 2 Pb and 2 Ti atoms each. The symmetry of this model is described by the tetragonal space group $P\bar{4}m2$ (D_{2d}^5 , No. 115), where the tetragonal

unit cell has half the volume of the cubic F -centered cell with lattice constants $a_t = b_t \approx a_c/\sqrt{2}$ and $c_t \approx a_c$, where the subscripts refer to tetragonal and cubic lattice constants, respectively. The transformation of coordinates from cubic to tetragonal unit cells is given by

$$\begin{pmatrix} x \\ y \\ z \end{pmatrix}_t = \begin{pmatrix} 1 & 1 & 0 \\ -1 & 1 & 0 \\ 0 & 0 & 1 \end{pmatrix} \cdot \begin{pmatrix} x \\ y \\ z \end{pmatrix}_c$$

Starting values for the fit in $P\bar{4}m2$ were obtained by applying this transformation to best fit values for atomic coordinates in $F43m$. Pb and Ti were placed at 4j and 4k, respectively, Nb at 4j and 4k, and oxygens at 4h, 4i, 2e, 2f, 8l, 2g, and 2g. The special oxygen O' in the structure may be placed at 1a (0, 0, 0) and 1c ($\frac{1}{2}$, $\frac{1}{2}$, $\frac{1}{2}$), where each O' atom is tetrahedrally coordinated either by all Pb or all Ti atoms, or at 2g[(0, $\frac{1}{2}$, z), ($\frac{1}{2}$, 0, \bar{z}), $z \approx \frac{1}{4}$] where each O' atom is coordinated by a mixture of two Pb and two Ti atoms. In order to resolve this ambiguity a refinement was done in which 1/2 oxygen per formula unit was initially distributed equally between the twofold site at 2g and the two onefold sites at 1a and 1c with the constraint that the stoichiometries for these sites sum to 1/2. All other crystallographic parameters were unconstrained. The fitting converged to a final result that placed 90% of this special oxygen on the twofold site and the remainder on the two onefold sites. A second fitting was done in which the special oxygen was constrained to remain on the two onefold sites with 1/4 oxygen per formula unit on each site. This refinement tended to diverge. These results show a clear preference for placing the special oxygen at 2g where it is coordinated by a mixture of two Pb and two Ti atoms. Consequently, the oxygen vacancies at 1a and 1c are coordinated by all like atoms in an irregular tetrahedral configuration with site symmetry $\bar{4}2m$.

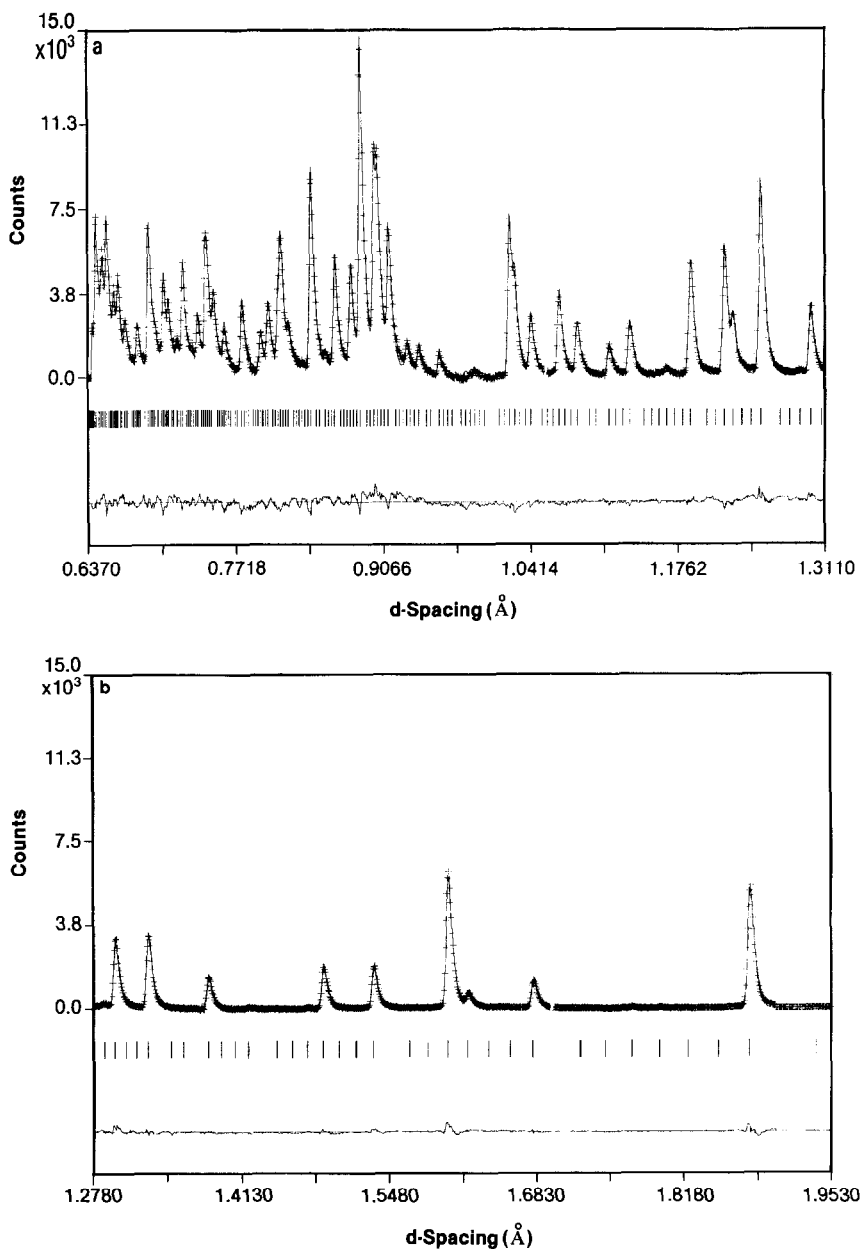


FIG. 5. (a,b,c,d) Refinement profile for $\text{PbTiNb}_2\text{O}_{6.5}$ in tetragonal $P\bar{4}m2$ (No. 115). The format is the same as for Fig. 2.

In a final fitting, the special oxygen was placed on the $2g$ site and its occupation as well as the Pb occupation at $4j$ and the Ti occupation at $4k$ was varied in the refinement. The refinement included 2776 data

points, 807 allowed reflections, and 39 refined parameters including the tetragonal cell constants and occupation factors as just described and isotropic temperature factors for all atoms. The refinement profile

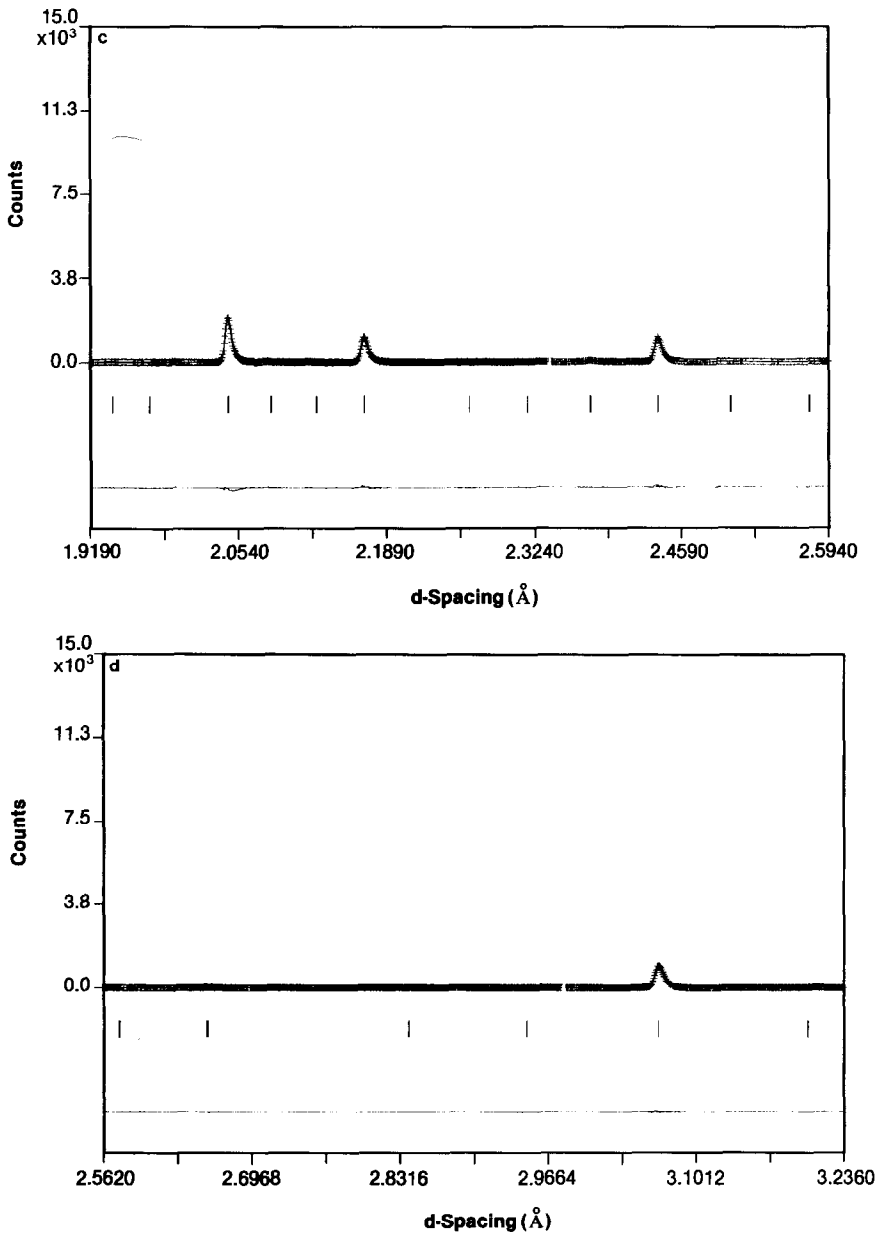


FIG. 5—Continued.

of the diffraction data, including all d -spacings between 0.631 and 3.218 \AA , is shown in Fig. 5, and the refinement results are summarized in Table III. The weighted profile R -value was 4.69% and the Rietveld R was 8.56%. The results show that there is

0.43(2) oxygen per formula unit on the defect site in agreement with the result for the fit in $F\bar{4}3m$ of 0.46(2) oxygen per formula unit on this site. For the oxygens comprising the corner-shared network of oxygen octahedra, the Nb—O bond lengths range

TABLE III
STRUCTURAL PARAMETERS FOR $\text{PbTiNb}_2\text{O}_{6.5}$ IN $P4m2$ WITH ORDERED OXYGEN VACANCIES, ORDERED Pb, Ti

$(a_t = 7.5104(5), c_t = 10.6250(14) \text{ \AA}) R_{\text{weighted}} = 4.69\%, R_{\text{Rietveld}} = 8.56\%, R_{\text{expected}} = 2.23\%$

| Atom | Site | Stoichiometry | x | y | z | B (\AA^2) |
|-----------------|--|---------------|---------------|---------------|---------------|-------------------------|
| Pb | 4j (x,0,z) | 0.98(2) | 0.749(1) | 0 | 0.872(1) | 1.69(6) |
| Ti | 4k ($x, \frac{1}{2}, z$) | 0.90(2) | 0.269(1) | $\frac{1}{2}$ | 0.376(1) | 1.69(6) |
| Nb | 4j (x,0,z) | 1 | 0.752(1) | 0 | 0.377(1) | 0.79(10) |
| Nb | 4k ($x, \frac{1}{2}, z$) | 1 | 0.253(1) | $\frac{1}{2}$ | 0.872(1) | 0.64(9) |
| O ₁ | 4h (x,x,0) | 1 | 0.308(1) | 0.308(1) | 0 | 0.30(16) |
| O ₂ | 4i ($x, x, \frac{1}{2}$) | 1 | 0.814(1) | 0.814(1) | $\frac{1}{2}$ | 0.28(15) |
| O ₃ | 2e (0,0,z) | $\frac{1}{2}$ | 0 | 0 | 0.311(2) | 0.54(29) |
| O ₄ | 2f ($\frac{1}{2}, \frac{1}{2}, z$) | $\frac{1}{2}$ | $\frac{1}{2}$ | $\frac{1}{2}$ | 0.822(2) | 1.02(35) |
| O ₅ | 8l (x,y,z) | 2 | 0.677(1) | 0.811(1) | 0.256(1) | 0.70(11) |
| O ₆ | 2g ($0, \frac{1}{2}, z$) | $\frac{1}{2}$ | 0 | $\frac{1}{2}$ | 0.548(1) | 0.98(23) |
| O ₇ | 2g ($0, \frac{1}{2}, z$) | $\frac{1}{2}$ | 0 | $\frac{1}{2}$ | 0.933(2) | 0.98(23) |
| O ₈ | 2g ($0, \frac{1}{2}, z$) | 0.43(2) | 0 | $\frac{1}{2}$ | 0.247(2) | 2.07(18) |
| O ₉ | 1a (0,0,0) | 0 | | | | |
| O ₁₀ | 1c ($\frac{1}{2}, \frac{1}{2}, \frac{1}{2}$) | 0 | | | | |

from 1.930(5) to 2.054(5) Å with an average Nb—O bond distance of 1.99 Å. This compares well with the Nb—O bond lengths of 1.98(1) and 2.00(1) Å found in the $F43m$ fit and with the Nb—O bond lengths of 2.01(2) and 1.97 Å in $\text{Ti}_2\text{Nb}_2\text{O}_6$ (16) and $\text{Pb}_{1.5}\text{Nb}_2\text{O}_{6.5}$ (21, 22), respectively. For the special oxygen, the Pb—O' bond distance, 2.27(2) Å, is in good agreement with the Pb—O' bond distance of 2.260(2) Å in $\text{Pb}_2\text{Ru}_2\text{O}_{6.5}$ (Table I) and 2.29 Å in $\text{Pb}_{1.5}\text{Nb}_2\text{O}_{6.5}$ (17–22). The Ti atom is significantly displaced toward its associated vacancy, as illustrated in Fig. 6, with the result that the Ti-vacancy distance of 2.16(1) Å, is significantly less than the Ti—O' distance 2.46(2) Å. This results in Ti—Ti separations of 3.47(2) and 3.60(2) Å, which are among the shortest Ti—Ti distances observed in compounds and in the element.

The $P4m2$ refinement results summarized in Table III show a positive difference ($c_t - \sqrt{2} a_t$) of about 2 standard deviations indicating a small tetragonal distortion of the cubic unit cell. A fitting in which the first

two cycles of refinement were forced to utilize values for a_t and c_t giving the same unit cell volume but a negative value for ($c_t - \sqrt{2} a_t$) ≈ -0.004 Å showed a tendency to wander slightly in subsequent cycles and did not return to positive values for ($c_t - \sqrt{2} a_t$). This result represented a false minimum since the weighted profile R -factor of 5.45% and Rietveld R of 10.70% for this fit were each significantly higher than the cor-

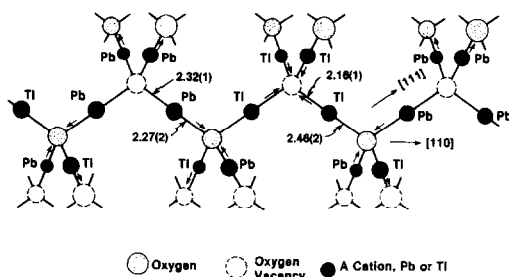


FIG. 6. $\text{PbTiO}_{0.5}$ sublattice in $\text{PbTiNb}_2\text{O}_{6.5}$ showing Pb, Ti, and oxygen vacancy ordering in $P4m2$. Arrows indicate the direction of displacement of Pb and Ti atoms with respect to the A-site position in $Fd3m$. Distances are given in Ångstroms.

responding values, 4.69 and 8.56%, given in Table III for the best $P4m2$ fit. Thus, the case for tetragonal symmetry rests on evidence for unit cell distortion as well as evidence for atomic ordering.

The Tl occupation of 0.90(2) implies a 10% Tl deficiency that appeared as an overall 4% A-site deficiency for the $F43m$ fit using Pb and Tl atoms disordered on the A-site. This apparent Tl deficiency is consistent with the observed oxygen stoichiometry of the defect site, 0.43(2), so that the correct formulation for this material is $\text{PbTi}_{0.90}\text{Nb}_2\text{O}_{6.45}$. Observations made during initial attempts to synthesize this material yield additional evidence for Tl deficiency. These early syntheses, which involved solid state reaction in ambient atmosphere at temperatures ranging from 500 to 900°C, yielded materials that did not exhibit a (420) reflection. Furthermore, as the temperature of synthesis was increased, a corresponding decrease in the lattice parameter of the product pyrochlore was observed. Coincident with this lattice parameter decrease, the relative intensities of the all-odd (hkl) reflections (cubic indexing) in the X-ray spectra decreased. These observations suggest that volatility of Tl prevented the synthesis of a product phase with the intended stoichiometry. A decrease in Tl content on the A-site would result in decreased intensity for all-odd (hkl) reflections in the X-ray spectra since Tl is a strong scatterer, and since the primary contribution to the intensities of these reflections is the difference in scattering power between A and B cations. The highest temperature of synthesis, 900°C, resulted in the formation of a pyrochlore phase whose lattice parameter was in agreement with literature values given for $\text{Pb}_{1.5}\text{Nb}_2\text{O}_{6.5}$ (17–22), thereby suggesting total loss of Tl by volatilization. Attempts to avoid loss of Tl by lowering the reaction temperature were not successful. Even at temperatures as low as 600°C, a gradual de-

crease in lattice parameter with time could be detected. Reaction temperatures significantly lower than 600°C resulted in poor product crystallinity and incomplete reaction.

Only under sealed-tube conditions could the intended stoichiometry be more nearly preserved which, in turn, gave rise to a (420) X-ray reflection. Nevertheless, even under sealed-tube conditions, it seems reasonable to expect that small amounts of Tl are lost to the vessel walls, thus yielding materials of less than ideal stoichiometries.

Conclusions

The defect pyrochlores $\text{Pb}_2\text{Ru}_2\text{O}_{6.5}$ and $\text{PbTi}_{0.90}\text{Nb}_2\text{O}_{6.45}$ show oxygen vacancy ordering that is accompanied by cation displacement in both cases. The traditional pyrochlore space group $Fd3m$, which requires the A-site to possess inversion center symmetry, can not be correct for either material. The neutron diffraction data for $\text{Pb}_2\text{Ru}_2\text{O}_{6.5}$ have been successfully fit in the cubic space group $F43m$. The results confirm half occupancy of the anion defect site, demonstrate oxygen vacancy ordering and show that each Pb atom is displaced by 0.040(4) Å toward its associated vacancy. The diffraction data for $\text{PbTiNb}_2\text{O}_{6.5}$ have been fit in the tetragonal space group $P4m2$ using a model that allows ordering of Pb and Tl on the A-site in concert with oxygen vacancy ordering. The results of this refinement, summarized in Table III, show that this model is superior to the model incorporating disordered Pb and Tl ($F43m$, Table II), is consistent with the expectation that Pb and Tl will not show equivalent displacement, and account for the presence of a (110) reflection in the diffraction data. The refinement results specify a stoichiometry $\text{PbTi}_{0.90}\text{Nb}_2\text{O}_{6.45}$; the slight Tl deficiency is probably associated with some loss of Tl during the sealed tube synthesis at 600°C.

Based on the present work we suggest

that oxygen vacancy ordering may be a frequently encountered phenomenon for oxygen defect pyrochlores with post-transition metal cations such as Tl^+ , Pb^{2+} , or Bi^{3+} on the *A*-site. For both $Pb_2Ru_2O_{6.5}$ and $PbTl_{0.90}Nb_2O_{6.45}$, oxygen vacancy ordering occurs in concert with *A*-site cation ordering. In the case of the latter material, the *A*-site ordering includes cation displacement both toward and away from the vacancy. The largest *A*-site atom displacement is exhibited in the $P\bar{4}m2$ refinement results for $PbTl_{0.90}Nb_2O_{6.45}$ (Table III) which show *Tl*-vacancy and *Tl*—*O'* distances of 2.16(1) and 2.46(2) Å, respectively. The resulting *Tl*—*Tl* separations, 3.47(2) and 3.60(2) Å are similar to those found in hcp *Tl* metal, 3.41 and 3.46 Å (23). We suggest that the *A*-site cation displacements that lead to the close *A*—*A* separations observed in these two materials are a consequence of *A* cation—oxygen bonding rather than formation of *A*—*A* bonds through the oxygen vacancy (5). The $P\bar{4}m2$ refinement of the diffraction data for $PbTl_{0.90}Nb_2O_{6.45}$ showed that the *Pb* atom is displaced slightly *away* from its associated oxygen vacancy, resulting in a *Pb*—*O'* bond distance of 2.27(2) Å which is equivalent to that found in $Pb_2Ru_2O_{6.5}$. However, the *Pb*-vacancy distance of 2.32(1) Å for this material is significantly larger than the *Pb*-vacancy distance 2.180(2) found in $Pb_2Ru_2O_{6.5}$. This suggests that the *Pb*—*O'* bonding requirement and not *Pb*—*Pb* bonding is driving the displacement of the *Pb* atom in each material. By similar reasoning the *Tl* atom is expected to be displaced *toward* its associated vacancy, for, if it were not, the resulting *Tl*⁺—*O'* bond length of 2.30 Å or less would be nearly equivalent to the *Tl*³⁺—*O* bond distance in oxide materials containing six- or eight-coordinate *Tl*³⁺. For example, Tl_2O_3 , which has the *C*— M_2O_3 structure with $a_0 = 10.54$ Å can be viewed as a defect fluorite in which each *Tl* atom has six equidistant *O* neighbors at 2.28 Å. The *Tl*³⁺-containing

material $Tl_2Ru_2O_7$ has been reported to be a pyrochlore (24) with $a_0 = 10.20(1)$ Å, space group $Fd\bar{3}m$, and therefore each *Tl*³⁺ atom has two equidistant *O* neighbors at 2.21 Å. Although it is well known that the size of cations such as *Tl*⁺, *Pb*²⁺, or *Bi*³⁺ depends on the degree of $6s^2$ lone-pair character (25), there is no evidence for a *Tl*⁺—*O* bond distance as short as 2.30 Å, a value comparable to typical *Tl*³⁺—*O* bond lengths. Thus displacement of the *Tl*⁺ atom in $PbTl_{0.90}Nb_2O_{6.45}$ *toward* its adjacent vacancy appears necessary in order to satisfy the *Tl*—*O'* bonding requirement and is probably not associated with the formation of *Tl*—*Tl* bonds. While the charge density associated with the $6s^2$ core electrons on *Tl*⁺ or on *Pb*²⁺ in $Pb_2Ru_2O_{6.5}$ or in $PbTl_{0.90}Nb_2O_{6.45}$ is expected to show significant *p* character (5, 15) and may well reside in the vicinity of the oxygen vacancy for coulombic reasons, there is no compelling evidence to support the concept of bond formation through the lone pair electrons in the vacancy, despite the close *Tl*—*Tl* separations observed in the latter compound.

To our knowledge these are the first examples of anion/vacancy ordering in a defect pyrochlore of the type $A_2B_2O_{7-y}$. This is not surprising since the reflections indicating oxygen vacancy ordering are quite weak and the associated *A*-site cation displacement, as in $Pb_2Ru_2O_{6.5}$, can be quite small. Finally, previous structure investigations of $Pb_2Ru_2O_{6.5}$ and similar systems (5, 21) relied solely on X-ray powder diffraction which is not as sensitive as neutron diffraction to the defect structure of the anion lattice. Reinvestigation of other oxygen defect pyrochlores with lone-pair cations on the *A*-site (5, 26, 27) would likely show oxygen vacancy ordering. In fact, reexamination of the X-ray spectrum of $Pb_2Ir_2O_{7-y}$, recently synthesized by the authors, shows the existence of a (420) reflection, suggesting an ordered, half occupancy of the special anion site.

Acknowledgments

The authors gratefully acknowledge Mr. H. J. Brady and Mr. J. T. Lewandowski for technical assistance in the synthesis and characterization of the materials reported here. The operation of the IPNS facility and the work of two of the authors (JDJ and FJR) are supported by the U.S. Department of Energy.

References

1. H. S. HOROWITZ, J. M. LONGO, AND J. T. LEWANDOWSKI, *Mater. Res. Bull.* **16**, 489 (1981).
2. H. S. HOROWITZ, J. M. LONGO, AND H. H. HOROWITZ, *J. Electrochem. Soc.* **130**, 1851 (1983).
3. H. H. HOROWITZ, H. S. HOROWITZ, AND J. M. LONGO, in "Proceedings, Symposium on Electrocatalysis" (W. E. O'Grady, P. N. Ross, and F. G. Will, Eds.), Vol. 82-2, The Electrochemical Society (1982).
4. J. J. RANDALL AND R. WARD, *J. Amer. Chem. Soc.* **81**, 2629 (1959).
5. J. M. LONGO, P. M. RACCAH, AND J. B. GOODENOUGH, *Mater. Res. Bull.* **4**, 191 (1969).
6. R. A. BEYERLEIN, H. S. HOROWITZ, J. M. LONGO, J. D. JORGENSEN, AND F. J. ROTELLA, in "Neutron Scattering—1981," AIP Conf. Proc. No. 89, (J. Faber, Jr., Ed.), p. 78, Amer. Inst. of Phys., New York (1982).
7. A. W. SLEIGHT, *Inorg. Chem.* **7**, 1704 (1968).
8. ZING P' was the prototype of the new pulsed neutron source, IPNS-I, a national user facility which commenced operation in 1981. J. M. Carpenter, *Nucl. Instrum. Methods* **145**, 91 (1977).
9. J. D. JORGENSEN AND F. J. ROTELLA, *J. Appl. Crystallogr.* **15**, 27 (1982).
10. R. B. VON DREELE, J. D. JORGENSEN, AND C. G. WINDSOR, *J. Appl. Crystallogr.* **15**, 581 (1982).
11. J. D. JORGENSEN AND J. FABER, JR., in "ICANS-VI, Proceedings, of the Sixth International Collaboration on Advanced Neutron Sources, Argonne National Laboratory, June 28–July 2, 1982" (J. M. Carpenter, Ed.) (ANL-82-80), p. 105 (1983).
12. B. S. BROWN, J. M. CARPENTER, J. D. JORGENSEN, D. L. PRICE, AND W. A. KAMITAKAHARA, in "Novel Materials and Techniques in Condensed Matter," (G. W. Crabtree and P. Vashishta, Eds.), pp. 311–340, Elsevier/North-Holland, Amsterdam/New York (1982).
13. The attempts to synthesize $\text{Pb}_2\text{Ru}_2\text{O}_6\text{F}$ included: (1) evacuated sealed tube reactions employing stoichiometric amounts of PbF_2 , PbO , PbO_2 , and RuO_2 ; (2) crystal growth in a PbO – PbF_2 eutectic flux; (3) hydrothermal crystallization of the flux grown products using an over pressure of HF.
14. A. DESCHANVRES, C. MICHEL, AND B. RAVEAU, *Bull. Soc. Chim.* **9**, 4805 (1968).
15. N. RAMADASS, T. PALANISAMY, J. GOPALAKRISHNAN, G. ARAVAMUDAN, AND M. V. C. SASTRI, *Solid State Commun.* **17**, 545 (1975).
16. J. L. FOURQUET, G. ORY, G. GAUTHIER, AND R. DE PAPE, *C.R. Acad. Sci. Paris, Serie C* **271**, 773 (1970).
17. W. R. COOK AND H. JAFFE, *Phys. Rev.* **89**, 1297 (1953).
18. R. S. ROTH, *J. Res. Nat. Bur. Stand.* **62**, 27 (1959).
19. V. S. KEMMLER-SACK AND W. RUDORFF, *Z. Anorg. Allg. Chem.* **344**, 23 (1966).
20. H. BERNOTAT-WULF AND W. HOFFMANN, *Naturwissenschaften* **67**, 141 (1980).
21. H. G. SCOTT, *J. Solid State Chem.* **43**, 131 (1982).
22. M. T. VANDENBORRE AND E. HUSSON, *Mater. Res. Bull.* **17**, 1289 (1982).
23. L. PAULING, "The Nature of the Chemical Bond," 3rd Edition, p. 410, Cornell Univ. Press, Ithaca, N.Y. (1960).
24. A. W. SLEIGHT AND J. L. GILLSON, *Mater. Res. Bull.* **6**, 781 (1971).
25. R. D. SHANNON, *Acta Crystallogr. A* **32**, 751 (1976).
26. R. J. BOUCHARD AND J. L. GILLSON, *Mater. Res. Bull.* **6**, 669 (1971).
27. O. MULLER, W. B. WHITE, AND R. ROY, *J. Inorg. Nucl. Chem.* **26**, 2075 (1964).